Identification of autoantibody clusters that best predict lupus disease activity using glomerular proteome arrays

Quan Li Zhen,[1] Chun Xie,[1] Tianfu Wu,[1] Meggan Mackay,[2] Cynthia Aranow,[2] Chaim Putterman,[3] and Chandra Mohan[1]

[1]Department of Internal Medicine — Rheumatology, Center for Immunology, University of Texas Southwestern Medical Center, Dallas, Texas, USA. [2]Division of Rheumatology, Columbia Presbyterian Medical Center, New York, New York, USA. [3]Division of Rheumatology, Albert Einstein College of Medicine, New York, New York, USA.

Nephrophilic autoantibodies dominate the seroprofile in lupus, but their fine specificities remain ill defined. We constructed a multiplexed proteome microarray bearing about 30 antigens known to be expressed in the glomerular milieu and used it to study serum autoantibodies in lupus. Compared with normal serum, serum from B6.*Sle1.lpr* lupus mice (C57BL/6 mice homozygous for the NZM2410/NZW allele of *Sle1* as well as the *FAS*^{lpr} defect) exhibited high levels of IgG and IgM antiglomerular as well as anti–double-stranded DNA/chromatin Abs and variable levels of Abs to α-actinin, aggrecan, collagen, entactin, fibrinogen, hemocyanin, heparan sulphate, laminin, myosin, proteoglycans, and histones. The use of these glomerular proteome arrays also revealed 5 distinct clusters of IgG autoreactivity in the sera of lupus patients. Whereas 2 of these IgG reactivity clusters (DNA/chromatin/glomeruli and laminin/myosin/Matrigel/vimentin/heparan sulphate) showed association with disease activity, the other 3 reactivity clusters (histones, vitronectin/collagen/chondroitin sulphate, and entactin/fibrinogen/hyaluronic acid) did not. Human lupus sera also displayed 2 distinct IgM autoantibody clusters, one reactive to DNA and the other apparently polyreactive. Interestingly, the presence of IgM polyreactivity in patient sera was associated with reduced disease severity. Hence, the glomerular proteome array promises to be a powerful analytical tool for uncovering novel autoantibody disease associations and for distinguishing patients at high risk for end-organ disease.

Introduction

Renal disease is a leading cause of mortality in murine and human lupus, and autoantibodies constitute important contributors to renal damage in this disease (1). In particular, anti-DNA and glomerulophilic Abs have been accorded a pathogenic role in this disease (2–8). Adoptive transfer studies of purified mAbs and hybridomas have revealed that whereas anti-histone and anti-nucleosome Abs may not be pathogenic, anti–double-stranded DNA (anti-dsDNA) and antiglomerular Abs may be pathogenic (9–12). In particular, correlative evidence and adoptive transfer studies have appended a greater degree of pathogenic potential to antiglomerular autoantibodies than to nonglomerular binding anti-DNA Abs (3, 10–12). Using conventional immunoassays, several investigators have highlighted the potential importance of Abs specific for various glomerular or basement membrane antigens (Ags) as being the targets for such antiglomerular, or "nephrophilic," autoantibodies. These Ags include laminin, various types of proteoglycans, heparin, collagen, α-actinin, etc. (13–28). In some instances, these antiglomerular reactivities have been demonstrated to be dependent upon nuclear Ag bridges, whereas in other studies, the nephrophilic Abs have been shown to be anti-DNA Abs with direct crossreactive potential to glomerular Ags (3, 9, 22–31). In addition, antiglomerular Abs that were not DNA reactive have also been documented in murine and human lupus nephritis (32, 33).

In contrast to the above studies, which focus on a couple of selected glomerular target Ag specificities, the recent advent of large-scale immunoproteomic approaches has allowed the screening of disease sera in a more comprehensive manner, against a vast array of potential target Ags (34–39). In particular, Robinson et al. have fabricated autoantigen microarrays, in which a large spectrum of autoantigens was spotted onto glass slides (40–42). Sera can then be added to these slides and developed with fluorescent-labeled secondary Abs to uncover the spectrum of antigenic specificities targeted in different autoimmune disease states. The purpose of the present study was to adopt a similar multiplexed approach to define the spectrum of autoantibodies reactive with different glomerular or glomerular basement membrane (GBM) Ags, which best correlate with disease activity and may be present in lupus. To this end, a panel of Ags documented to be present in the glomeruli/GBM (43–45) was spotted onto specially precoated glass slides; these arrays have been termed *glomerular proteome arrays*. These novel proteome microarrays were then used to analyze the nephrophilic autoantibody profiles in murine and human lupus.

Interestingly, lupus mice were noted to harbor a wide spectrum of antibodies, including autoantibodies to α-actinin, aggrecan, collagen, entactin, fibrinogen, hemocyanin, heparan sulphate, laminin, myosin, proteoglycans, DNA, and histones. In addition, the use of these arrays has also helped to uncover 2 nonoverlapping IgG autoantibody clusters that distinguish lupus patients with more severe disease activity.

Nonstandard abbreviations used: Ag, antigen; B6, C57BL/6; Cy, cyanine; dsDNA, double-stranded DNA; GBM, glomerular basement membrane; GN, glomerulonephritis; nfi, normalized fluorescence intensity unit(s); SLE, systemic lupus erythematosus; SLEDAI score; SLE disease activity score; Sm/RNP, Smith Ag/ribonucleoprotein; ssDNA, single-stranded DNA.

Conflict of interest: The authors have declared that no conflict of interest exists.

Citation for this article: *J. Clin. Invest.* **115**:3428–3439 (2005). doi:10.1172/JCI23587.

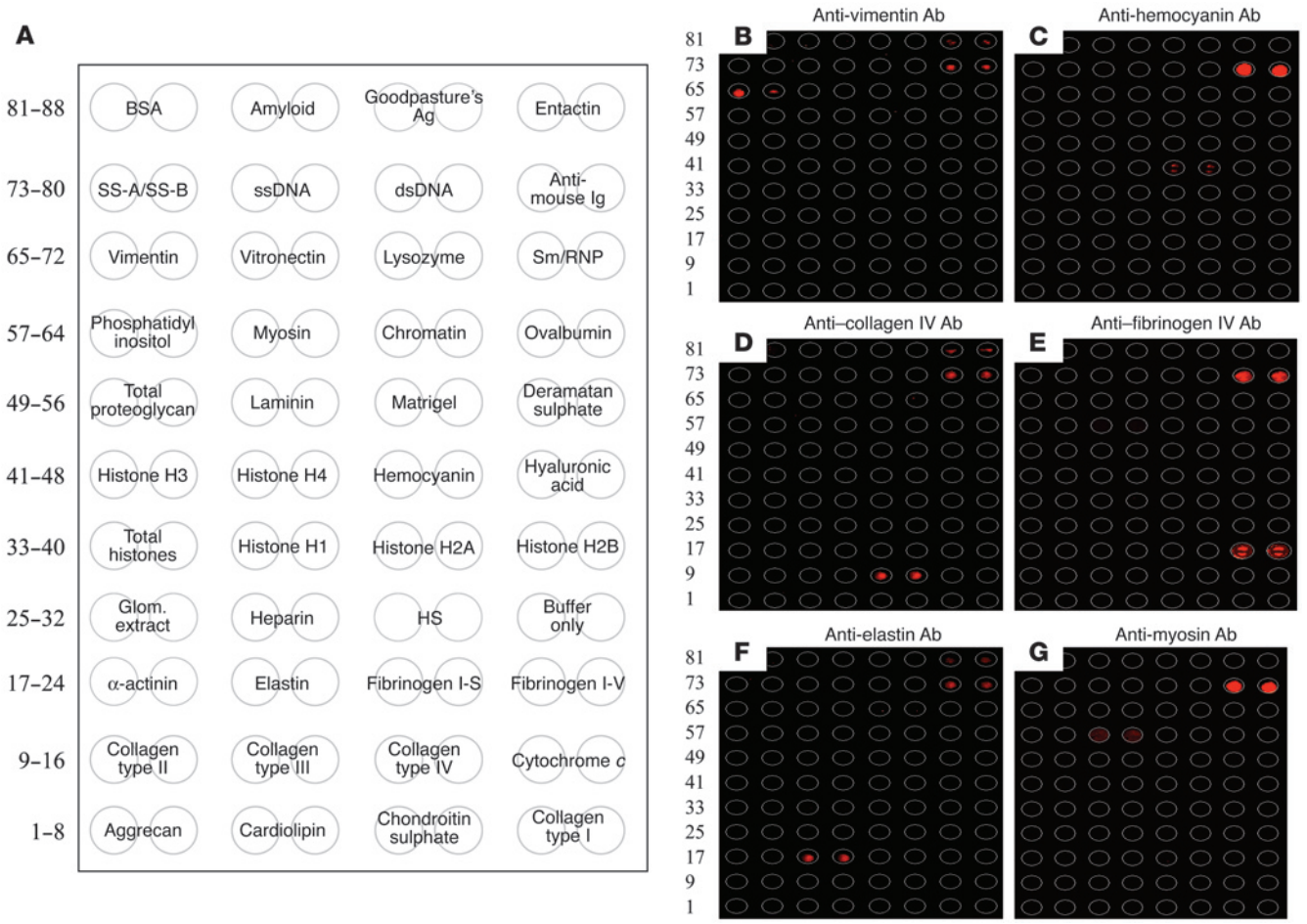

Figure 1
Target Ags and specificity profiles of glomerular proteome arrays. (**A**) HydroGel slides were coated with different glomerular/GBM and nuclear Ags in duplicate as shown. Deramatan sulphate, deramatan sulphate proteoglycan; glom. extract, glomerular extract; HS, heparan sulphate. (**B**–**G**) Six commercially available mAbs specific for vimentin (**B**), hemocyanin (**C**), collagen IV (**D**), fibrinogen IV (**E**), elastin (**F**), and myosin (**G**) were added to 6 separate glomerular proteome arrays and developed using Cy5-labeled goat anti-mouse IgG/IgM in order to gauge the specificity of the Ag/Ab interactions on the glomerular proteome arrays. The Ags in **B**–**G** were arrayed as shown in **A**.

Results

First, a panel of glomerular/GBM Ags as well as control nuclear Ags was assembled as shown on the array map portrayed in Figure 1A. The initial studies were focused on selecting the optimal slide chemistry for Ag spotting. The panel of Ags assembled did not bind well to untreated glass slides, but adhered fairly well to poly-L-lysine, superaldehyde, and HydroGel coated slides. Among the different slide surface chemistries tested, HydroGel coated slides yielded the best results in terms of the evenness and consistency of the spot dimensions as well as the signal-to-noise ratios, as illustrated in Supplemental Figure 1A (supplemental material available online with this article; doi:10.1172/JCI23587DS1). We also verified that whereas the omission of a blocking step resulted in high-fluorescence background, preincubating the slides in PBS, 0.1% Tween 20, and 0.5% BSA yielded optimal blocking, as depicted in Supplemental Figure 1B. Next, each Ag was spotted at 4 serial dilutions (from 0.025 to 1 μg/ml) to determine the optimal coating concentration for each Ag, as exemplified in Supplemental Figure 1C. For almost all Ags, the optimal signal-to-noise ratios were observed when 1 μg/ml was used for coating. An exception was cardiolipin, for which the optimal coating concentration was noted to be 0.1 μg/ml. Hence, all further studies were performed using HydroGel slides coated with the different Ags at the optimal coating concentrations.

Next, we titrated the test sera and commercially available mAbs of defined specificities to ascertain the dynamic performance range of the arrays and their sensitivities. The titration curve for the anti-elastin mAb is depicted in Supplemental Figure 2A and is compared with the corresponding ELISA readings observed at the same dilutions (Supplemental Figure 2B). It was clear that diluting the mAb more than 25,000-fold yielded an array signal that was still significantly above the background; in contrast, diluting the mAb beyond 3,000-fold dropped the OD values to the ELISA background levels. Similar titration curves were derived using 5 additional mouse mAbs as well as lupus sera. Whereas the arrays performed significantly better than the conventional ELISA approach in the case of the anti-elastin and anti-myosin Abs (in being able to detect reactivity at far lower Ab dilutions), the anti-vimentin, anti–collagen IV, anti-hemocyanin, and anti–fibrinogen IV mAbs performed similarly in both the ELISA and array methodologies (data

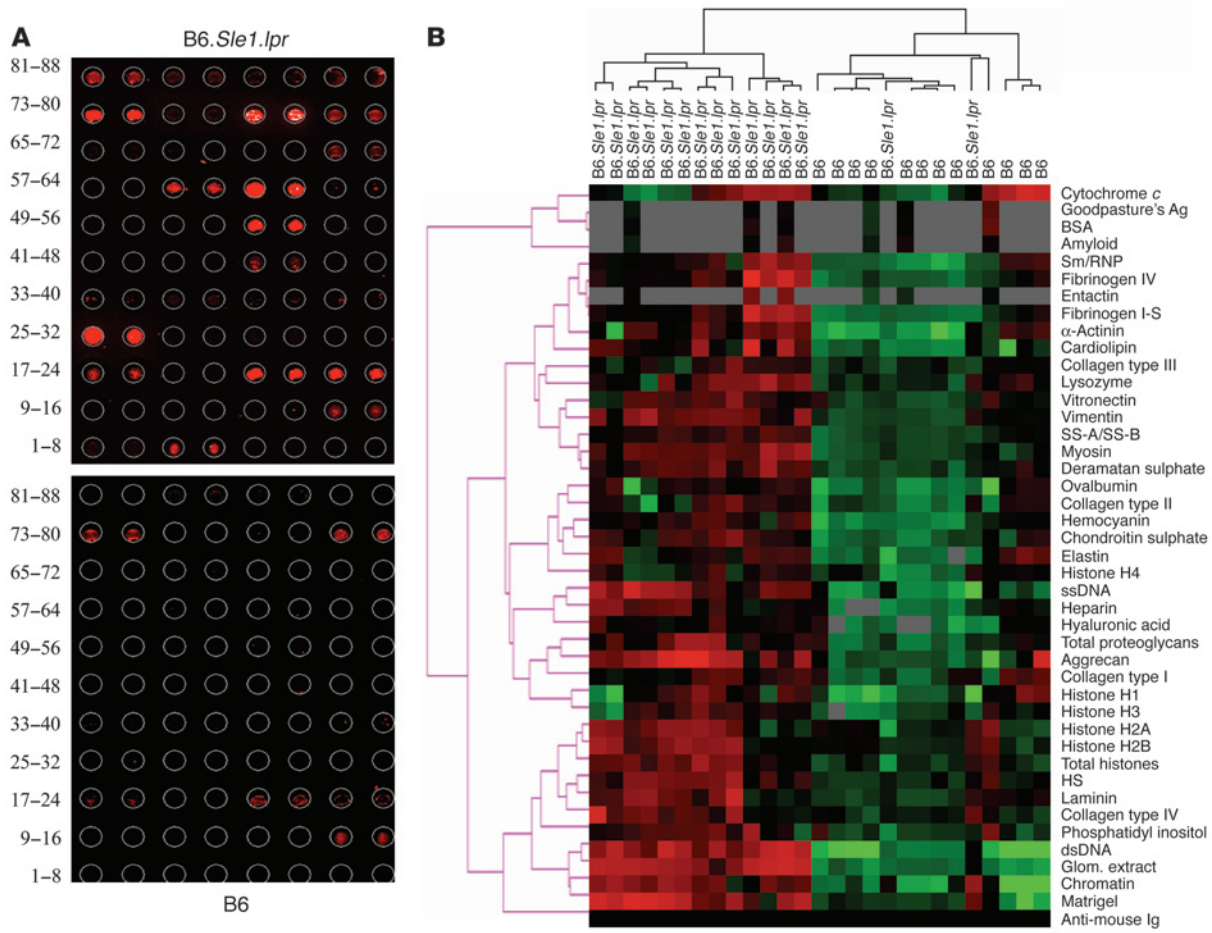

Figure 2

The use of glomerular proteome arrays to uncover autoantibodies in murine lupus sera. Dilutions (1:200) of various sera were applied to HydroGel slides coated with different glomerular/GBM and nuclear Ags as shown in Figure 1A. (**A**) Representative glomerular proteome arrays hybridized with B6 (bottom) or B6.*Sle1.lpr* sera (top) and developed with Cy5-coupled anti-mouse IgG. In these arrays, the intensity of the fluorescence signal ranged from none (black) to high (red), as scanned at 635 nM. (**B**) A total of 12 B6 sera and 15 B6.*Sle1.lpr* sera (10 females, 5 males) were studied similarly, and the data summarized in a heat map which shows the relative IgG seroreactivities of each of these 27 serum samples to the respective Ags on the arrays. For all Ags, the reactivity intensities are depicted on a relative scale, where reactivities above the array mean are colored red, reactivities below are colored green, and reactivities close to the mean are colored black. In addition, a clustering algorithm was used to group together sera that exhibited similar reactivity patterns (dendrogram at top) and to cluster together Ags that were similarly targeted by the different test sera (dendrogram at left). Data in **B** are representative of at least 3 independent experiments (using the same sera, but independent arrays).

not shown). Likewise, as portrayed in Supplemental Figure 2C, serum from B6.*Sle1.lpr* lupus mice (C57BL/6 mice homozygous for the NZM2410/NZW allele of *Sle1* as well as the *FAS*^{lpr} defect) showed significant IgG and IgM reactivity to dsDNA, chromatin, and several glomerular Ags, even when diluted beyond 25,000-fold. Hence, the glomerular proteome array appears to be particularly sensitive, with a significant dynamic range, yielding a fairly linear readout spanning 4 logs of fluorescence intensity and corresponding to 4–5 logs of Ab dilution.

The specificity of the assay was next gauged using commercially available mAbs. Figure 1, B–G, depicts the Ag specificity profiles of 6 commercially available mouse mAbs, with specificities for vimentin, hemocyanin, collagen IV, fibrinogen IV, myosin, and elastin. All 6 Abs reacted specifically with their target Ags but not with the other Ags on the arrays, with 1 exception. Interestingly, some of the tested Abs demonstrated a low degree of binding to the entactin preparation, perhaps reflecting the presence of some contaminating proteins in the entactin preparation. Reactivity to the mouse Ig spotted on all arrays served as a positive control and also allowed for interslide normalization.

Having optimized the slide precoating chemistry, Ag coating concentrations, Ab/serum dilutions to use, and the specificity and sensitivity profiles of the array, sera from a healthy mouse strain and sera drawn from a lupus-afflicted strain were compared with respect to their reactivity profiles to the different glomerular Ags. For this purpose, we selected C57BL/6 (B6) mice as the negative control and B6.*Sle1.lpr* as the disease strain, since they both share the same genetic background but differ vastly in their clinical phenotypes. Importantly, B6.*Sle1.lpr* mice are known to exhibit highly penetrant lupus nephritis, accompanied by high titers of anti-DNA and antiglomerular Abs (46). With both sets of sera, negligible reactivity was observed against the control Ags

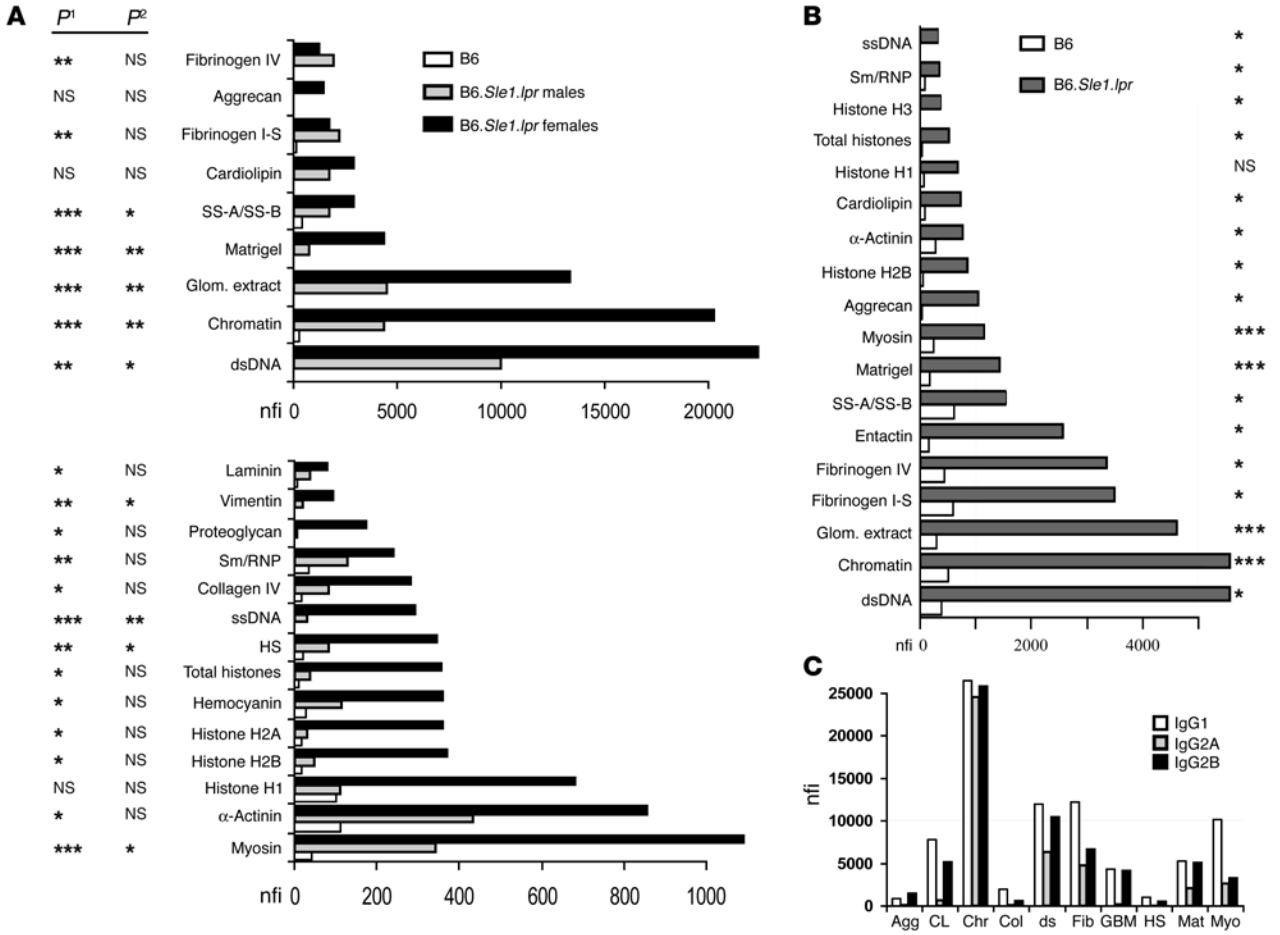

Figure 3

The strongest IgG and IgM antiglomerular reactivities in B6.*Sle1.lpr* lupus sera. (**A**) IgG seroreactivities to various glomerular and nuclear Ags assayed in B6 (n = 12) and B6.*Sle1.lpr* mice (n = 15, 10 females and 5 males) are partitioned according to whether the observed reactivities in the lupus sera were stronger than 1,000 nfi (top) or 100–1,000 nfi (bottom). Among the B6 sera, there were no significant differences between genders; therefore data from B6 males and females have been pooled. P values at left compare B6.*Sle1.lpr* with the corresponding B6 values (P^1) and differences between gender in B6.*Sle1.lpr* sera (P^2). *P < 0.05; **P < 0.01; ***P < 0.001. Note that the reactivity levels of B6.*Sle1.lpr* female sera to chromatin and dsDNA exceeded 20,000 nfi. (**B**) The strongest IgM seroreactivities (>300 nfi) noted in 15 B6.*Sle1.lpr* sera (10 females, 5 males) using glomerular proteome arrays are compared with the corresponding B6 levels (n = 12). P values at right compare the 2 strains. (**C**) Some of the highest fluorescence reactivities observed in B6.*Sle1.lpr* sera, categorized according to their IgG subclass. In similar assays, the reactivities observed in B6 control sera ranged from 20–100 nfi (data not plotted). Agg, aggrecan; CL, cardiolipin; Chr, chromatin; Col, collagen type IV; ds, dsDNA; Fib, fibrinogen IV; GBM, total glomerular lysate; Mat, Matrigel; Myo, myosin.

ovalbumin and lysozyme as well as against the spots that were coated with no Ags, which typically yielded 10–60 normalized fluorescence intensity units (nfi). In contrast, the lupus sera, but not the control sera, reacted strongly to several glomerular and nuclear Ags, as illustrated in Figure 2A; indeed, the sera from these 2 strains clustered apart from each other almost perfectly, as illustrated by the heat map in Figure 2B.

Among the B6.*Sle1.lpr* lupus sera, the strongest autoreactivity was noted against dsDNA, chromatin, total glomerular sonicate, and the Matrigel mix of basement membrane Ags; these can be seen tightly clustered toward the bottom of the heat map in Figure 2B. In particular, the reactivities to dsDNA, chromatin, and total glomerular sonicate ranged from 10,000–30,000 nfi in female B6.*Sle1.lpr* lupus mice (Figure 3A). Weaker but significant reactivity (>1,000 nfi) was also noted against fibrinogen, cardiolipin, aggrecan, and SS-A/SS-B (also known as Ro/La Ags) in lupus, but not control, sera (Figure 3A). Compared with the B6 sera, the lupus sera also exhibited stronger reactivities against myosin, α-actinin, collagen IV, hemocyanin, and heparan sulphate as well as the nuclear Ags, single-stranded DNA (ssDNA), and histones, though these signals were somewhat weaker (100–1,000 nfi; Figure 3A). Reactivity to most of the other glomerular Ags examined (e.g., the other collagens, hyaluronic acid, etc.) was either absent or barely above the background. Interestingly, most of the observed seroreactivities were significantly higher in B6.*Sle1.lpr* females compared with males (Figure 3A), as has been noted previously (46).

The presence of serum IgM autoantibodies was also examined. As depicted in Figure 3B, the strongest reactivity was again noted against dsDNA, chromatin, and total glomerular sonicate in lupus sera but not control sera. Weaker but significant levels of IgM autoantibodies were also noted against the same subset of Ags targeted by the IgG Abs, including α-actinin, aggrecan, car-

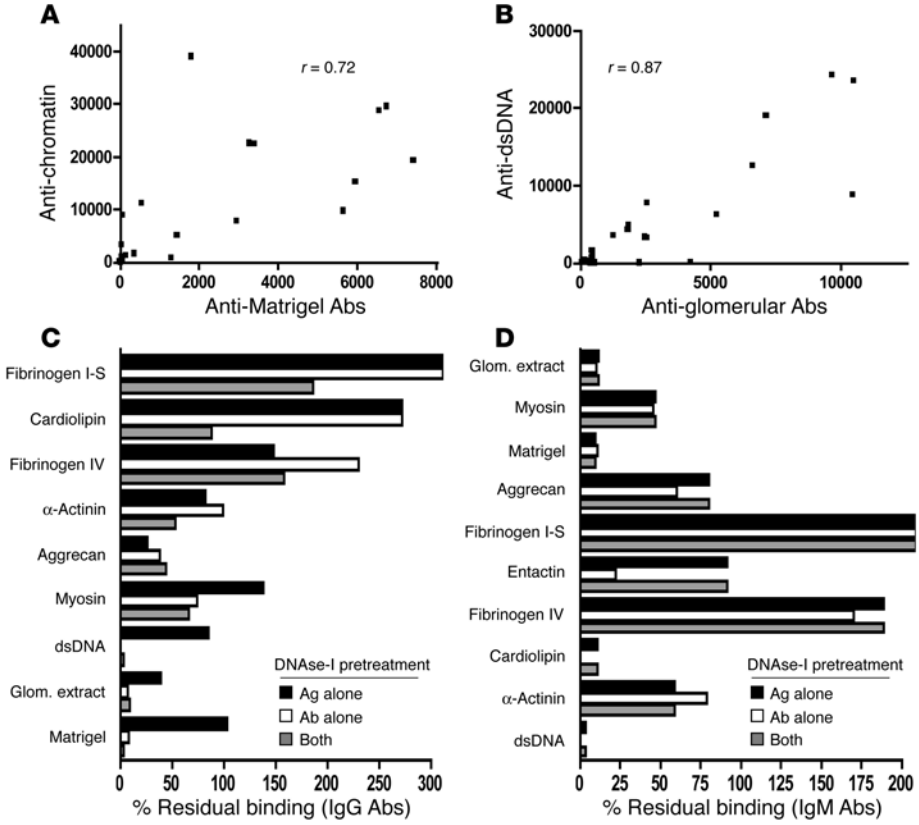

Figure 4
DNA dependence of glomerular-reactive autoantibodies in lupus. For all the B6 and B6.*Sle1.lpr* mouse sera studied (total, $n = 27$; **A** and **B**), the reactivity to DNA/chromatin was compared to the reactivities to total glomerular lysate or Matrigel, within the same serum samples. Shown are the scatter plots (and correlation coefficients) relating mouse IgG reactivities against chromatin versus Matrigel (**A**) and mouse IgM reactivity against dsDNA versus glomerular extract (**B**). (**C** and **D**) Mean remnant IgG (**C**) and IgM (**D**) seroreactivities to dsDNA or to the different glomerular Ags following DNAse-I pretreatment of the glomerular proteome array slides, the test sera alone, or both, expressed as a percentage of the fluorescence intensities recorded in sham-treated controls, arbitrarily set at 100%. Each bar represents the mean value derived from 3 individual B6.*Sle1.lpr* serum samples that had expressed high reactivity to the depicted glomerular targets. All IgG seroreactivities remaining after both the sera and the Ag arrays were DNAse-I treated (**C**) were significantly less than the sham-treated controls ($P < 0.05$ for fibrinogen IV; $P < 0.01$ for myosin; and $P < 0.001$ for all the other Ags), with the exception of α-actinin ($P > 0.05$). Likewise, all IgM seroreactivities remaining after both the sera and the Ag arrays were DNAse-I treated (**D**) were significantly less than the sham-treated controls ($P < 0.01$ for aggrecan and $P < 0.001$ for the other Ags), with the exceptions of fibrinogen IV and α-actinin ($P > 0.05$).

diolipin, fibrinogen, and myosin. Unlike the IgG autoantibodies, no difference was noted in IgM autoantibody levels between the genders in B6.*Sle1.lpr* sera except in the levels of various antihistone specificities (data not shown).

The utility of the glomerular proteome array was extended to study the isotype subclasses of antiglomerular Abs. The simultaneous use of cyanine 3–coupled (Cy3-coupled) anti-mouse IgG1 and Cy5-coupled anti-mouse IgG2A (or anti-mouse IgG2B) to develop the slides allowed us to quantitate the relative amounts of glomerular Ag-specific Abs of different isotypes in any given serum sample. As depicted in Figure 3C, B6.*Sle1.lpr* sera exhibited high levels of IgG1, IgG2B, and IgG2A Abs to various targets, including dsDNA and chromatin. Consistent with the data shown in Figure 3A, B6 sera showed negligible levels of Abs to these Ags (data not shown).

The above findings indicate that lupus sera harbor IgM and IgG reactivities to several nuclear as well as GBM Ag preparations. The fact that the total glomerular sonicate and the Matrigel preparations represented relatively crude Ag mixes, as well as the observation that the reactivities to these complex antigenic mixes were closely paralleled by their respective strengths of reactivity to chromatin/DNA (Figure 3), triggered us to examine this further. Indeed, when the reactivity profile of each individual control as well as lupus mouse serum was analyzed, a strong correlation was observed between the antinuclear reactivity and the antiglomerular reactivity in both the IgG and the IgM Abs (Figure 4, A and B). We next examined whether the observed reactivity profiles to the glomerular Ags were mediated at least in part by residual, or contaminating, nuclear material in the glomerular/Matrigel preparations or within the Ag-binding pockets of the serum Abs. To directly test this, the immunoproteome assays were repeated after DNAse-I pretreatment of the glomerular proteome array slides alone, the lupus sera alone, or both components.

DNAse-I pretreatment of the lupus sera reduced IgG and IgM binding to the glomerular lysates and Matrigel by >80% (Figure 4, C and D), indicating that the DNA dependence of the glomerular reactivity was largely due to DNA-bearing Ags bound within the serum Abs. Although DNAse-I pretreatment abrogated antiglomerular reactivity, it was interesting to observe that the reactivity to certain Ags, such as fibrinogen, was unaltered or even increased following DNAse-I pretreatment. On the other hand, IgG reactivity to α-actinin, myosin, and aggrecan were partially impaired by the DNAse-I pretreatment of the sera and slides (Figure 4C), indicating that not all target Ag specificities are absolutely DNA dependent. An almost identical pattern was observed when the DNA dependence of IgM autoantibodies was examined — whereas reactivity to glomerular sonicates and Matrigel were almost obliterated and reactivity to fibrinogen was paradoxically elevated, the reactivity to α-actinin, myosin, and aggrecan were partially impaired (Figure 4D).

The usefulness of the arrays in studying patient samples was next evaluated. Figure 5 shows the IgG seroreactivities to the different glomerular and nuclear Ags noted in normal human sera ($n = 11$), sera from lupus patients with varying degrees of disease activity ($n = 37$; Table 1), and sera from 5 RA controls.

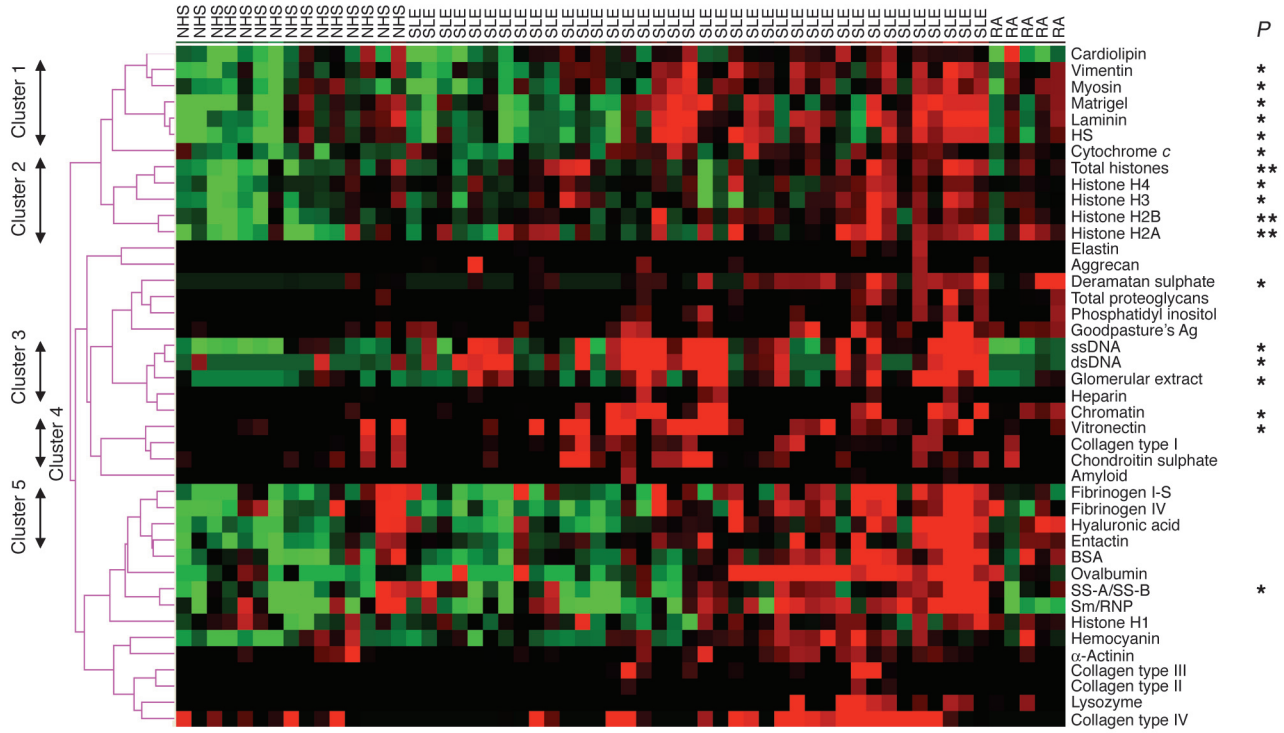

Figure 5
The strongest IgG antiglomerular reactivities in human lupus sera. Sera from 11 healthy adults (NHS), 37 lupus patients (SLE) with varying degrees of disease (see Table 1), and 5 RA patients were applied to the glomerular proteome arrays as shown in Figure 1A and developed using Cy5-labeled anti-human IgG. The relative fluorescence intensities for each Ag are depicted using a green/black/red heat map and clustered Ag-wise as described in the legend to Figure 2B. Indicated on the left margin are 5 distinct groups of Ags, the reactivities to which were noted to cluster together in the tested samples. Depicted results are representative of 2 independent experiments using the same sera but fresh arrays. *P* values indicated at right were the result of comparing the lupus sera against the normal controls. An additional SLE column has been included which shows results from 1 duplicated sample. $^{*}P < 0.05$; $^{**}P < 0.01$.

It was evident from the heat map in Figure 5 that the sera from lupus patients exhibited significantly higher levels of IgG Abs to several different nuclear and glomerular Ags compared with sera from RA patients and healthy adults. Even more striking was the uncovering of 5 or more Ag reactivity clusters, shown along the left margin in Figure 5. To confirm the clustering tree automatically generated by the Cluster/TreeView algorithm (http://rana.lbl.gov/EisenSoftware.htm) in Figure 5, pairwise correlations were next performed for the different Ags tested using Excel software (Microsoft Office 2003; Microsoft). As denoted in Figure 6, A–E, 5 distinct IgG autoantibody clusters surfaced, marked by a high degree of correlation between the Ab specificities within each cluster (with r typically exceeding 0.6 between any 2 given specificities; Figure 6, A–E), and low correlation ($r < 0.2$) among Ab specificities drawn from different clusters.

Reactivity to vimentin, myosin, Matrigel, laminin, and heparan sulphate clustered together (Figure 6A), whereas reactivity to the different core histones (but not histone H1) clustered separately (Figure 6B). Reactivity to DNA-bearing Ags (ssDNA, dsDNA, and chromatin), as well as to total glomerular lysate, clustered together (Figure 6C). Reactivity to chondroitin sulphate, collagen I, and vitronectin clustered somewhat weakly (Figure 6D), whereas reactivity to entactin, hyaluronic acid, and the fibrinogens clustered together strongly (Figure 6E). In contrast to these clusters, reactivity to the other Ags studied displayed unique distribution profiles, with the exception of SS-A/SS-B and Smith Ag/ribonucleoprotein (Sm/RNP), which displayed concordant seroreactivity profiles in the study subjects as shown in Figure 5.

We next asked whether the above reactivity clusters were useful in distinguishing lupus patients with differing disease activity. Interestingly, cluster 1 reactivity (IgG anti-laminin, anti-myosin, etc.) and cluster 3 reactivity (anti-DNA, antiglomerular Abs) were significantly higher in patients with higher total systemic lupus erythematosus (SLE) disease activity scores (SLEDAI scores; Figure 6, F and H) as well as higher renal SLEDAI scores (data not shown). In contrast, cluster 2, cluster 4, and cluster 5 specificities failed to distinguish patients with low SLEDAI scores from those with high disease activity (Figure 6, G, I, and J). When cluster 1 and cluster 3 specificities were examined further, it was interesting to note that a substantial fraction of patients with high IgG autoantibody levels had grade III or IV glomerulonephritis (GN), but not grade V GN (Figure 6, F and H, and Table 1). Interestingly, of the 3 patients with grade IV GN (based on past biopsy reports) but low total SLEDAI scores, 2 were free of active renal disease; therefore, the levels of cluster 1 and cluster 3 seroreactivities appeared to correlate better with concurrent renal disease/flares rather than past history of pathology. When the absolute SLEDAI scores (or any of the other disease parameters listed in Table 1) were used as continuous variables to ascertain correlation with any of the Abs assayed, only the cluster 3 specificities (e.g., anti-dsDNA,

Table 1
Human subjects studied using glomerular proteome arrays

Subject ID	Age (yr)	Ethnicity/ gender	Total SLEDAI	Renal SLEDAI	ANA titer	Anti-dsDNA (AU)	Serum C3 (AU)	Serum C4 (AU)	Protein/ Cr ratio	GN score[A]
Sle1	54	H/F	12	12	>640	14	113	57	2.3	IV (–29[B])
Sle2	29	H/M	12	12	>160	18	102	38	9.1	IV
Sle4	33	H/F	5	4	160	10	77	23	3.2	
Sle5	29	H/F	20	16	160	138	67	1	4.7	IV (0[B])
Sle6	33	B/F	12	8	640	138	107	15	0.8	II, III (–7[B])
Sle13	50	H/F	0	0	80	1	121	49	–	
Sle14	31	B/F	16	12	320	167	99	8	1.6	III (–20[B])
Sle16	28	H/M	16	0	160	>500	36	8	–	
Sle17	56	H/F	8	4	160	6	75	16	1.1	V (0[B])
Sle18	42	B/F	8	4	640	36	33	<8	0.6	
Sle19	20	B/F	14	8	320	115	89	<8	–	
Sle21	32	B/F	10	8	320	22	81	13	1.8	III + V (–3[B])
Sle23	56	H/F	0	0	80	4	144	24	–	
Sle24	56	H/F	6	0	>640	13	104	10	–	
Sle26	26	H/F	8	8	0	32	112	35	3.9	IV, VI, sclerosis (–21[B])
Sle27	57	B/F	0	0	>320	28	160	42	–	
Sle28	54	W/F	0	0	>640	68	117	32	0.1	
Sle29	57	H/F	0	0	>640	14	206	26	–	
Sle31	15	B/F	5	4	0	8	97	16	0.1	IV (–10[B])
Sle32	35	B/F	16	12	>640	206	48	<8	1.2	IV (–21[B])
Sle43	35	B/F	0	0	80	25	145	20	–	
Sle45	31	B/F	0	0	320	32	88	16	0.0	
Sle46	33	H/F	0	0	160	13	105	37	–	
Sle48	29	B/F	0	0	320	1	108	26	0.0	
Sle53	27	H/F	18	16	320	14	115	16	10.9	IV, sclerosis (–2[B])
Sle69	49	H/F	4	4	0	19	112	26	1.8	Vb (–23[B])
Sle70	46	H/F	2	0	320	31	67	17	–	
Sle71	39	B/F	18	12	0	4	96	18	3.2	V (–2[B])
Sle89	35	B/F	0	0	80	56	137	21	–	
Sle104	49	H/M	2	0	80	13	66	23	–	ESRD on hemodialysis
Sle110	20	H/F	19	12	NA	141	68	11	0.8	
Sle112	31	B/F	2	0	NA	21	76	8	0.4	
Sle113	28	B/F	2	0	NA	32	80	20	0.1	IV (–29[B])
Sle115	55	H/F	0	0	0	5	129	17	0.2	
Sle116	31	H/F	18	12	640	>200	86	13	2.3	III (–2[B])
Sle120	41	B/F	0	0	640	5	117	53	0.1	
Sle132	39	H/F	2	0	320	10	152	25	0.1	
RA23	69	B/F	NA	NA	0	0	132	23	NA	
RA24	61	H/F	NA	NA	0	0	142	30	NA	
RA25	67	B/F	NA	NA	0	3.3	133	23	NA	
RA38	47	H/F	NA	NA	0	NA	115	42	NA	
RA42	59	H/F	NA	NA	0	NA	NA	NA	NA	
NC1	26	I/F	NA	NA	NA	NA	NA	NA	NA	
NC2	52	H/F	NA	NA	NA	NA	NA	NA	NA	
NC3	26	C/F	NA	NA	NA	NA	NA	NA	NA	
NC5	52	B/F	NA	NA	NA	NA	NA	NA	NA	
NC7	54	B/F	NA	NA	NA	NA	NA	NA	NA	
NC9	48	W/F	NA	NA	NA	NA	NA	NA	NA	
NC11	27	W/F	NA	NA	NA	NA	NA	NA	NA	
NC12	27	W/F	NA	NA	NA	NA	NA	NA	NA	
NC33	48	B/F	NA	NA	NA	NA	NA	NA	NA	
NC36	34	B/F	NA	NA	NA	NA	NA	NA	NA	
NC39	31	W/F	NA	NA	NA	NA	NA	NA	NA	

The ANA, anti-dsDNA, C3, and C4 levels were assessed at about the same time that sera were drawn for the glomerular proteome array studies. [A]Histological GN was determined using the WHO scale. [B]Time interval (in months) between the preceding renal biopsy and the blood draw that was used for the glomerular proteome array studies. B, African-American; C, Chinese; F, female; H, Hispanic; I, Asian Indian; M, male; W, Caucasian; Cr, creatinine; ESRD, end-stage renal disease; NC, normal healthy control. Dashes indicate that no protein was detected in the urine.

antiglomerular Abs, etc.) showed a positive correlation with total SLEDAI score (r = 0.34; data not plotted) and a negative correlation with serum C3 (r = –0.41 for IgG anti-dsDNA; Figure 6K). Cluster 1 specificities, as well as the other specificities assayed on the arrays, did not correlate well with the absolute SLEDAI scores, proteinuria, or hypocomplementemia (data not shown).

Figure 7 shows the IgM seroreactivities to the different glomerular Ags in the same group of lupus patients and controls. In general, when the Ag reactivity profiles of all 53 study subjects were considered together, the IgM reactivity profiles to the different Ags demonstrated a fairly good correlation with their respective IgG reactivities. However, this was not because of any cross-reactivity of the anti-IgM detection Ab (see Methods) or because of rheumatoid factor, which was verified to be absent in most of the study subjects. Interestingly, however, in contrast to the IgG seroreactivities portrayed in Figure 5, the IgM reactivity displayed 2 broad clusters. On the one hand, IgM reactivity to ssDNA, dsDNA, and chromatin were strongly clustered together (Figure 7A). In contrast, about 60% of the Ags tested clustered together broadly (Figure 7A, arrow); this broad cluster included anti-histone Abs and reactivity to several control Ags such as lysozyme, BSA, and ovalbumin, indicating that these are likely to repre-

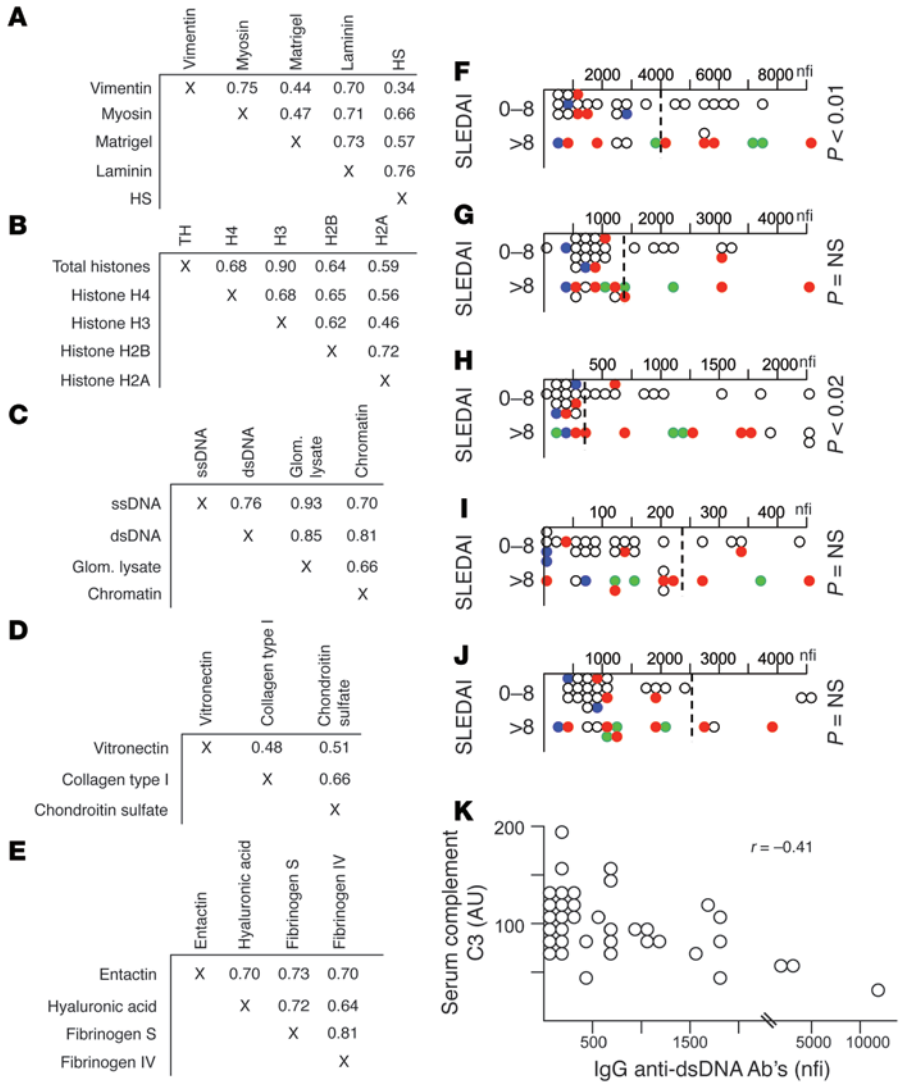

Figure 6

Five distinct clusters of IgG autoreactivity in lupus sera. (**A**–**E**) The autoantigen seroreactivities that apparently clustered together in Figure 5 were reassessed for correlation in a pairwise fashion. Indicated within each matrix are the corresponding correlation coefficients when seroreactivity to the different Ags were compared for concordance. For array Ags not listed in **A**, the seroreactivity correlation coefficients between any 2 Ags were $r < 0.2$, with the exception of concordance between SS-A/SS-B and Sm/RNP seroreactivity. (**F**–**J**) Seroreactivity levels noted in lupus sera ($n = 37$) against the 5 clusters of targeted Ags, parsed according to their total SLEDAI scores. When available, glomerular pathology class was indicated (red, grade IV GN; green, grade II/III GN; blue, grade V GN; white, no biopsy done). (**F**) For cluster 1 Ags, reactivity to laminin is plotted as the cluster's representative. (**G**) For cluster 2 Ags, reactivity to total histone is plotted as the cluster's representative. (**H**) For cluster 3 Ags, reactivity to dsDNA is plotted as the cluster's representative. (**I**) For cluster 4 Ags, reactivity to chondroitin sulphate is plotted as the cluster's representative. (**J**) For cluster 5 Ags, reactivity to fibrinogen IV is plotted as the cluster's representative. The dotted line within each plot pertains to the cutoff for normality, representing mean ± 2 SD noted in the 11 normal control sera studied. (**K**) Scatter-plotted serum concentrations of complement C3 (y axis) versus IgG anti-dsDNA Ab levels (representative of cluster 3 seroreactivity; x axis).

sent IgM polyreactive Abs. Interestingly, 3–4 of the RA patients also exhibited these polyreactive Abs in the absence of anti-DNA Abs (Figure 7A). Besides these 2 broad clusters, the other specificities in between were only weakly clustered together (Figure 7A).

We next asked how the degree of IgM anti-DNA reactivity and/or the extent of IgM polyreactivity correlated with disease. The former was represented by the average nfi for anti-ssDNA, anti-dsDNA, and anti-chromatin assayed for each sample, whereas the latter was represented by the mean nfi derived by averaging the IgM reactivity to the 26-Ag cluster described above (Figure 7A). Interestingly, whereas the healthy controls had low to modest levels of anti-DNA and polyreactive IgM Abs, RA patients had significantly higher levels of IgM polyreactive Abs (Figure 7B, black dots). Among SLE patients, it was intriguing to observe that patients with low disease activity (Figure 7B, blue dots) tended to have higher levels of IgM polyreactive Abs than patients with more severe active disease (Figure 7B, red dots), who tended to have higher levels of IgM anti-DNA Abs. Viewed from a different perspective, among SLE patients who possessed high serum IgM anti-DNA Abs, the copresence of IgM polyreactive Abs in their serum (Figure 7B, upper right quadrant) was associated with lower disease activity.

Discussion

This work contributes several novel perspectives to our understanding of antiglomerular Ab specificities in lupus. First and foremost, it allows for an unbiased comparison of different antiglomerular and antinuclear fine specificities in lupus nephritis in parallel. Since all specificities were assayed using the same conditions on the same slides and normalized in an identical manner, this allowed us to compare the relative levels of the different Ab specificities in a very reliable fashion. Through this parallel comparison using murine and human lupus sera, we observed that the reactivity to dsDNA and total glomerular lysate was far stronger than the reactivity to any of the other nuclear Ags — including ssDNA, histones, Sm/RNP, and SS-A/SS-B — or the other glomerular Ags tested. DNA/glomerular autoreactivity was not only profound in the sera from the lupus mice, it also constituted a distinct IgG autoantibody cluster that distinguished lupus patients with more severe disease activity and renal disease (Figure 6, H and K) from patients with low disease activity. Hence, these studies reaffirm the prominence and potential pathogenic significance of anti-dsDNA and antiglomerular Abs in lupus proposed in previous studies (2–12).

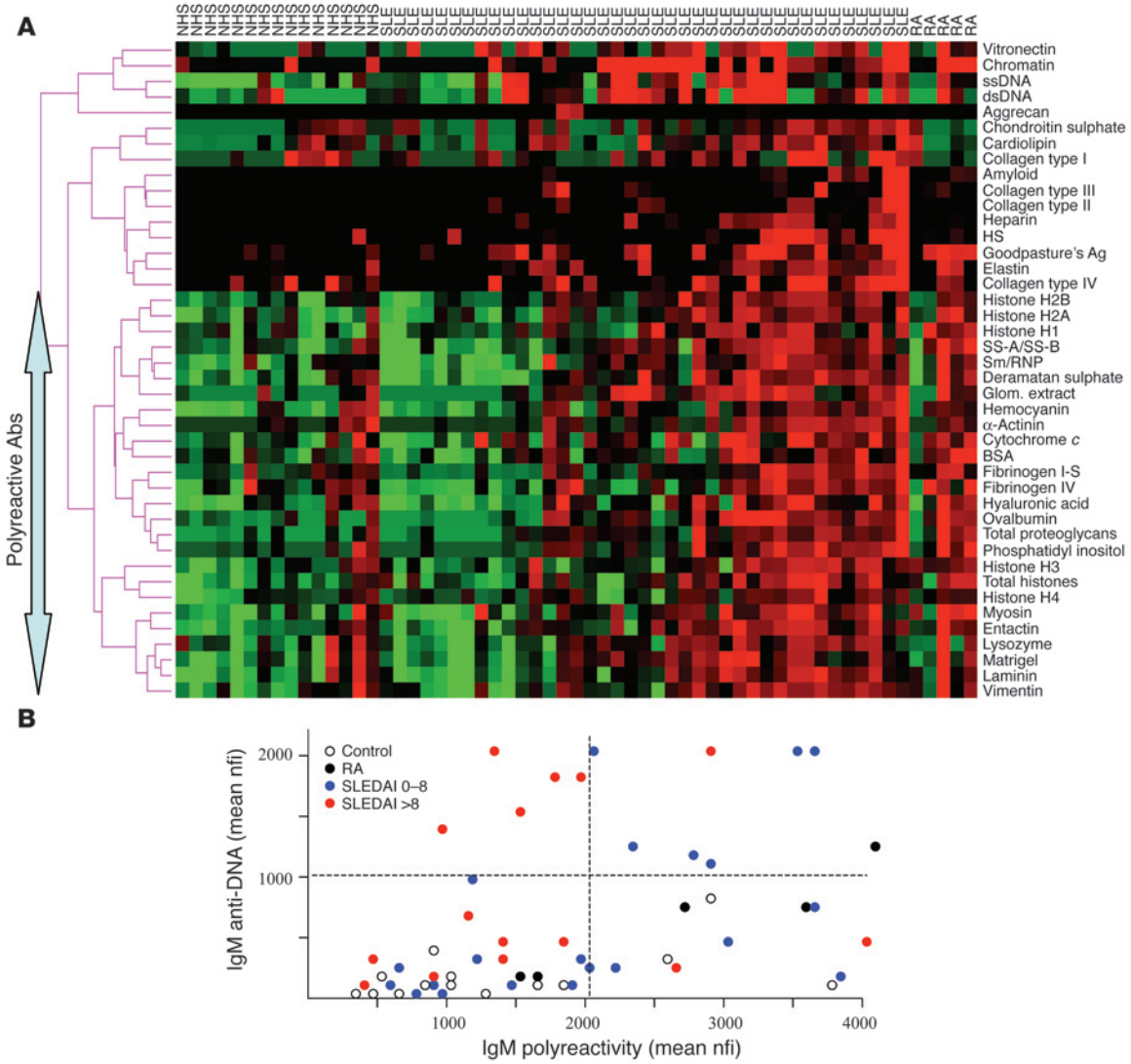

Figure 7

The strongest IgM antiglomerular reactivities in human lupus sera. (**A**) Sera from 11 healthy adults, 37 lupus patients with varying degrees of disease (see Table 1), and 5 RA patients were applied to the glomerular proteome arrays as shown in Figure 1A and developed using Cy3-labeled anti-human IgM. The relative fluorescence intensities for each Ag are depicted using a green/black/red heat map and clustered Ag-wise as described in the legend to Figure 2B. Indicated on the left are a panel of Ags that clustered together, most likely serving as targets for polyreactive Abs. Depicted results are representative of 2 independent experiments using the same sera but fresh arrays. Two additional SLE columns have been included which show results from 2 duplicated samples. (**B**) For each normal control (n = 11; white dots), RA control (n = 5; black dots), and lupus patient (n = 37; blue dots, total SLEDAI score 0–8; red dots, total SLEDAI score >8), the mean serum IgM anti-DNA reactivity (y axis) was derived by averaging the observed reactivity to ssDNA, dsDNA, and chromatin on the arrays and scatter plotted against the average extent of serum IgM polyreactivity (x axis) to the bottom-most 26 array Ags clustered together in the heat map shown in **A**. The dotted lines were arbitrarily set to distinguish patients with high IgM anti-DNA Abs and/or high IgM polyreactivity in their sera.

It was clear from the DNAse-I pretreatment studies that the majority of glomerular-reactive Abs were really anti-dsDNA (or anti-dsDNA/protein) Abs that had acquired nephrophilicity due to the nuclear material complexed within their Ag-binding pockets. This resonates well with previous reports demonstrating that nephrophilicity can be mediated by DNA-containing bridges (3, 11, 29–31). It was interesting, however, to observe that the reactivity to several of these glomerular/GBM Ags were only partially abrogated by DNAse-I pretreatment. A significant fraction of the reactivity to α-actinin, myosin, entactin, and aggrecan, for instance, appears to be independent of nuclear antigenic bridges. On the other hand, it remains possible that the observed "direct" binding to these Ags is mediated, at least in part, by anti-DNA Abs that are crossreactive to these other Ags, as has been demonstrated previously with a couple of glomerular Ags (22–29). It will be important to firmly establish the extent to which reactivity to these glomerular Ags is mediated by crossreactive anti-DNA Abs in future studies.

Both the DNAse-I pretreatment studies as well as the emergence of distinct autoantibody clusters in the lupus sera point to the importance of additional autoantibody specificities in lupus. A second important IgG autoantibody cluster uncovered using the glomerular proteome arrays was composed of laminin, myosin,

heparan sulphate, Matrigel, and vimentin (Figure 5 and Figure 6, A–E). Previous Ab transfer studies by other investigators (3, 13, 14, 16, 21–24), as well as the apparent association of this Ab cluster with more severe disease (Figure 6F), underline the potential pathogenic significance of these autoantibodies. Although anti-laminin, anti-myosin, and anti–heparan sulphate Abs have previously been implicated in lupus nephritis, vimentin constitutes a novel addition to this cluster. The inclusion of Matrigel in this cluster may not be a surprise, since laminin and heparan sulphate constitute 2 dominant constituents of Matrigel.

With both the above clusters (cluster 1 and cluster 3), these Abs were more prominent in patients with higher SLEDAI scores. Since almost all patients with SLEDAI scores greater than 8 also had significant renal SLEDAI scores, one can surmise that these autoantibody clusters may actually be reflective of renal flares. It would be important in future studies to examine how these clusters fluctuate in longitudinal studies and how they relate to the degree of renal pathology. Though some of the studied patients had biopsy information, these numbers were quite limited; clearly, these studies need to be expanded and confirmed in additional data sets.

Using the glomerular proteome arrays, this study has uncovered several additional IgG autoantibody clusters in lupus sera, including anti-histone Abs as well as several previously unreported specificities: vitronectin, collagen I, chondroitin sulphate, entactin, hyaluronic acid, fibrinogen, etc. However, these did not appear to associate with disease severity (Figure 6). An additional insight of this study revolves around the IgM autoantibody specificities in lupus. Whereas some lupus patients, as well as the B6.*Sle1.lpr* lupus mouse strain, possessed very high levels of IgM anti-DNA Abs, a substantial fraction of the lupus and RA patients were noted to possess IgM reactivity to a broad cluster of 26 Ags, including several foreign (control) Ags. This apparent polyreactivity was not simply the consequence of rheumatoid factors, since most of the patients and controls were verified to be negative for rheumatoid factors. Caution should, however, be exercised in labeling these Abs as being polyreactive, since it is still possible that these may indeed represent multireactivity rather than polyreactivity. Clearly, future absorption studies and examination at the monoclonal level will help make this distinction.

Assuming these are indeed polyreactive IgM Abs, our results lend support to 2 novel notions, both of which warrant further experimental verification. First, it appears that among patients with serum anti-DNA Abs, the co-presence of polyreactive IgM Abs in the serum may confer protection against disease (Figure 7B), although this needs to be formally demonstrated. This correlates well with the demonstrated protective role of IgM in lupus (47). Second, IgM polyreactivity appears to be a common denominator of several autoimmune diseases, including lupus and RA, even if these Abs are not directly pathogenic. This observation is consistent with the recent description of polyreactive Abs in the early repertoire of lupus and RA patients based on single-cell B cell repertoire studies (48, 49).

As illustrated in this study, immunoproteome arrays offered the advantage of massive multiplexing compared with conventional ELISA and Western blot approaches. Moreover, this approach also compares superbly to the latter approaches in terms of its sensitivity and specificity (34–40). Since 1 set of test samples can be Cy3-labeled, a second set Cy5-labeled, and both samples cohybridized onto the same substrate spots, the glomerular proteome arrays and similar target organ Ag arrays lend themselves handsomely to several additional comparisons: predisease versus disease-phase sera; IgM Abs versus IgG Abs to different end-organ targets; paired serum–renal eluate, serum-CSF, and serum–synovial fluid comparisons; etc. In addition, the panel of Ags spotted onto these arrays can be readily modified or expanded to examine the potential disease contribution of RNA/DNA-containing immune complexes as well as to study serum and/or fluids from related connective tissue diseases. The autoantigen proteome array originally introduced by Robinson and colleagues (40–42), together with the more focused tissue-targeted arrays such as the glomerular proteome array described in this study, are likely to expand our serodiagnostic horizon in the coming years.

Methods

Antigens. The literature was first surveyed to identify Ags that were known to be expressed in the glomerular milieu and/or GBM (43–45). Total glomerular sonicates were obtained by harvesting glomeruli from B6 mouse kidneys and sonicating them as described previously (46, 50). Total chromatin was prepared from sheep rbcs as described previously (51). Entactin (nidogen) and Goodpasture's Ag (the NC1 domain of collagen IV) were kind gifts from J. Wieslander (Lund University, Lund, Sweden). All other Ags were purchased from Sigma-Aldrich, INOVA Diagnostics Inc., BD Biosciences — Pharmingen, Roche Diagnostics, or Chondrex Inc. The optimal coating concentration for all Ags was determined to be 1 μg/ml except for cardiolipin, for which the optimal concentration was determined to be 0.1 μg/ml.

Slide manufacture. Ags were dissolved in PBS (or other buffers, as recommended by the manufacturer) and diluted from 1 μg/ml to 0.025 μg/ml using the "printing" buffer (0.06 M sodium bicarbonate, pH 9.5). Poly-L-lysine, super-aldehyde, or HydroGel coated slides were purchased from PerkinElmer. All slides were prewashed using PBS and double-deionized water (3 5-minute washes) and spin dried for storage. A BioRobotics MicroGrid II spotter (Genomic Solutions) was used to print the proteins in duplicate or triplicate onto the precoated slides. After printing, the slides were incubated in a humid chamber, rinsed with PBS, spin dried, and stored at 4°C.

Hybridization. On the day of hybridization, the Ag-coated slides were washed using 0.1% Tween-20 in PBS, blocked with wash buffer containing 0.5% BSA, rinsed, and spin dried. Up to 100 μl of the appropriately diluted serum sample (optimal dilution, 1:200) was applied to the slide, and slides were placed in a hybridization chamber at 37°C for 1 hour. The slides were then washed and spin dried. Cy3- or Cy5-labeled anti-IgM, anti-IgG and various isotype-specific detection Abs (5 μg/ml; Jackson ImmunoResearch Laboratories) were next applied to the slides. We verified that the anti-IgM detection Ab used did not crossreact with array-bound IgG. Following 1 hour of incubation at 37°C, the slides were washed and spin dried. Finally, the slides were scanned using a GenePix 4000B scanner (Molecular Devices). Whereas the Cy3 signal (green) was scanned at 532 nM, the Cy5 signal (red) was scanned at 635 nM. All fluorescence intensities were normalized using mouse/human total Ig (Sigma-Aldrich) spotted onto the same slide. To derive the nfi, the absolute fluorescence intensity against any given Ag was divided by the absolute fluorescence intensity for the Ig control spots, and the resulting ratio was multiplied by a factor of 1,000. For each Ag, data obtained from duplicate or triplicate spots were averaged prior to any statistical comparison.

Murine Abs and sera. The anti–collagen IV, anti-elastin, anti-hemocyanin, anti–fibrinogen IV, anti-myosin, and anti-vimentin mouse mAbs were purchased from Sigma-Aldrich, reconstituted to 1 mg/ml, and used to gauge the sensitivity and specificity of the glomerular proteome arrays. B6 mice were purchased from Jackson ImmunoResearch Laboratories. B6.*Sle1.lpr* mice, homozygous for the NZM2410/NZW allele of *Sle1* as well as the FAS^{lpr} defect, were bred in our animal facility; the lupus phenotypes in these mice have been described previously (52). Sera were

obtained from both strains at 6–9 months of age for use in this study. All animal studies were approved by the University of Texas Southwestern Medical School Animal Use Review Committee.

Patient recruitment and sera. Sera were drawn from 11 healthy adults who were seronegative for anti-DNA Abs, 5 RA patients, and 37 SLE patients at the Albert Einstein College of Medicine in accordance with institutional review board–approved guidelines. Subjects gave informed consent for the study. With regard to the SLE patients, all subjects who fulfilled at least 4 American College of Rheumatology criteria for diagnosis were recruited for the study. From this collection, blood samples from 37 patients were used for the glomerular proteome studies so as to include patients with a wide spread of SLEDAI scores (53). The age and ethnicity of the study subjects as well as their SLEDAI scores, ANA titers, ELISA-determined anti-DNA Ab levels, serum complements (C3 and C4 levels), and severity of renal inflammation graded using the WHO classification (54) are detailed in Table 1. Renal SLEDAI score was derived from the total SLEDAI score by totaling only the renal-specific components of the SLEDAI score. For some analyses, the patients were divided into 2 groups based on whether they had mild disease (SLEDAI score, 0–8) or more severe lupus (SLEDAI score, >8) based on the threshold used to classify severe lupus flares for which the SLEDAI scores typically exceed 12 (55, 56). For most patients, the time between clinical disease assessment and blood draw was 1 week. On the other hand, the kidney biopsy information presented in Table 1 was obtained 0–29 months prior to blood draw. Most patients were undergoing treatment for their disease; however, any potential impact of particular immunosuppressives on autoantibody titers or patterns were not specifically examined in this study.

DNAse-I pretreatment studies. For some of the depicted studies, either the human or mouse serum alone, the Ag-coated slides alone, or both were pretreated with DNAse-I for 30 minutes at 37°C, using 200 U/ml for treating the serum and 50 U/ml for treating the arrays (in buffer containing 50 mM Tris-HCl, 75 mM KCl, and 3 mM $MgCl_2$; pH 8.3) before hybridizing the sera to the slides. The resulting fluorescence intensities were expressed as a ratio relative to the fluorescence intensities derived using sham (PBS) pretreatment.

Data analysis. For intergroup comparisons, the Student's *t* test was used (SigmaStat version 2.0; Jandel Scientific). Heat map diagrams with row-wise and columnwise clustering were generated using Cluster and TreeView software (versions 2.2 and 1.6, respectively; http://rana.lbl.gov/EisenSoftware.htm). In these diagrams, fluorescence intensities that were higher than the row mean were colored red, those that fell below the row mean were colored green, and cells with signals close to the mean were left black. Missing data was denoted using gray.

Acknowledgments

This work was supported by grants from the NIH (R01 AI47460, to C. Mohan; R01 AR486912 and PO1 AI51392, to C. Putterman). We would also like to acknowledge Mei Yan and Desi Kresak for technical assistance, Ramesh Saxena for helpful feedback, and Jorgen Wieslander for his generous gift of antigens.

Received for publication October 11, 2004, and accepted in revised form October 3, 2005.

Address correspondence to: Chandra Mohan, Simmons Arthritis Research Center, Department of Internal Medicine — Rheumatology, University of Texas Southwestern Medical Center, Mail Code 8884, Y8.204, 5323 Harry Hines Boulevard, Dallas, Texas 75390-8884, USA. Phone: (214) 648-9675; Fax: (214) 648-7995; E-mail: Chandra.mohan@utsouthwestern.edu.

1. Kotzin, B.L. 1996. Systemic lupus erythematosus. *Cell.* **85**:303–306.
2. Hahn, B.H. 1998. Antibodies to DNA. *N. Engl. J. Med.* **338**:1359–1368.
3. Lefkowith, J.B., and Gilkeson, G.S. 1996. Nephritogenic autoantibodies in lupus. Current concepts and continuing controversies. *Arthritis Rheum.* **39**:894–903.
4. Foster, M.H., and Kelley, V.R. 1999. Lupus nephritis: update on pathogenesis and disease mechanisms. *Semin. Nephrol.* **19**:173–181.
5. Madaio, M.P., et al. 1987. Murine monoclonal anti-DNA antibodies bind directly to glomerular antigens and form immune deposits. *J. Immunol.* **138**:2883–2889.
6. Raz, E., Brezis, M., Rosenmann, E., and Eilat, D. 1999. Anti-DNA antibodies bind directly to renal antigens and induce kidney dysfunction in the isolated perfused rat kidney. *J. Immunol.* **142**:3076–3082.
7. Dang, H., and Harbeck, R.J. 1984. The in vivo and in vitro glomerular deposition of isolated anti-double-stranded-DNA antibodies in NZB/W mice. *Clin. Immunol. Immunopathol.* **30**:265–278.
8. Ehrenstein, M.R., et al. 1995. Human IgG anti-DNA antibodies deposit in kidneys and induce proteinuria in SCID mice. *Kidney Int.* **48**:705–711.
9. Limaye, N., and Mohan, C. 2004. Pathogenicity of anti-DNA/glomerular autoantibodies — weighing the evidence [review]. *Drug Discovery Today: Disease Models.* **1**:395–403.
10. Budhai, L., Oh, K., and Davidson, A. 1996. An in vitro assay for detection of glomerular binding IgG autoantibodies in patients with systemic lupus erythematosus. *J. Clin. Invest.* **98**:1585–1593.
11. Bernstein, K.A., Valerio, R.D., and Lefkowith, J.B. 1995. Glomerular binding activity in MRL lpr serum consists of antibodies that bind to a DNA/histone/type IV collagen complex. *J. Immunol.* **154**:2424–2433.
12. Liang, Z., et al. 2003. Pathogenic profiles and molecular signatures of ANAs derived from NZM2410 lupus mice. *J. Exp. Med.* **199**:381–398.
13. Kashihara, N., Makino, H., Szekanecz, Z., Waltenbaugh, C.R., and Kanwar, Y.S. 1992. Nephritogenicity of anti-proteoglycan antibodies in experimental murine lupus nephritis. *Lab. Invest.* **67**:752–760.
14. Foster, M.H., Liu, Q., Chen, H., Nemazee, D., and Cooperstone, B.G. 1997. Anti-laminin reactivity and glomerular immune deposition by in vitro recombinant antibodies. *Autoimmunity.* **26**:231–243.
15. Chugh, S., et al. 2001. Aminopeptidase A: a nephritogenic target antigen of nephrotoxic serum. *Kidney Int.* **59**:601–613.
16. Wick, G., Muller, P.U., and Timpl, R. 1982. In vivo localization and pathological effects of passively transferred antibodies to type IV collagen and laminin in mice. *Clin. Immunol. Immunopathol.* **23**:656–665.
17. Bhandari, S., Harnden, P., Brownjohn, A.M., and Turney, J.H. 1998. Association of anticardiolipin antibodies with intraglomerular thrombi and renal dysfunction in lupus nephritis. *QJM.* **91**:401–409.
18. Loizou, S., et al. 2000. Significance of anticardiolipin and anti-beta(2)-glycoprotein I antibodies in lupus nephritis. *Rheumatology.* **39**:962–968.
19. Yanase, K., Smith, R.M., Puccetti, A., Jarett, L., and Madaio, M.P. 1997. Receptor-mediated cellular entry of nuclear localizing anti-DNA antibodies via myosin 1. *J. Clin. Invest.* **100**:25–31.
20. Atta, M.S., Powell, R.J., Hopkinson, N.D., and Todd, I. 1994. Human anti-fibronectin antibodies in systemic lupus erythematosus: occurrence and antigenic specificity. *Clin. Exp. Immunol.* **96**:20–25.
21. Bruijn, J.A., et al. 1990. Characterization and in vivo transfer of nephritogenic autoantibodies directed against dipeptidyl peptidase IV and laminin in experimental lupus nephritis. *Lab. Invest.* **63**:350–359.
22. Sabbaga, J., Line, S.R., Potocnjak, P., and Madaio, M.P. 1989. A murine nephritogenic monoclonal anti-DNA autoantibody binds directly to mouse laminin, the major non-collagenous protein component of the glomerular basement membrane. *Eur. J. Immunol.* **19**:137–143.
23. Faaber, P., Rijke, T.P., van de Putte, L.B., Capel, P.J., and Berden, J.H. 1986. Cross-reactivity of human and murine anti-DNA antibodies with heparan sulfate. The major glycosaminoglycan in glomerular basement membranes. *J. Clin. Invest.* **77**:1824–1830.
24. Termaat, R.M., et al. 1990. Cross-reactivity of monoclonal anti-DNA antibodies with heparan sulfate is mediated via bound DNA/histone complexes. *J. Autoimmun.* **3**:531–545.
25. van Bruggen, M.C., et al. 1996. Heparin and heparinoids prevent the binding of immune complexes containing nucleosomal antigens to the GBM and delay nephritis in MRL/lpr mice. *Kidney Int.* **50**:1555–1564.
26. Mostoslavsky, G., et al. 2001. Lupus anti-DNA autoantibodies cross-react with a glomerular structural protein: a case for tissue injury by molecular mimicry. *Eur. J. Immunol.* **31**:1221–1227.
27. Deocharan, B., Qing, X., Lichauco, J., and Putterman, C. 2002. Alpha-actinin is a cross-reactive renal target for pathogenic anti-DNA antibodies. *J. Immunol.* **168**:3072–3078.
28. Mason, L.J., Ravirajan, C.T., Rahman, A., Putterman, C., and Isenberg, D.A. 2004. Is alpha-actinin a target for pathogenic anti-DNA antibodies in lupus nephritis? *Arthritis Rheum.* **50**:866–870.
29. Termaat, R.M., et al. 1992. Anti-DNA antibodies can bind to the glomerulus via two distinct mechanisms.

Kidney Int. **42**:1363–1371.
30. van Bruggen, M.C., et al. 1997. Antigen specificity of anti-nuclear antibodies complexed to nucleosomes determines glomerular basement membrane binding in vivo. *Eur. J. Immunol.* **27**:1564–1569.
31. Di Valerio, R., Bernstein, K.A., Varghese, E., and Lefkowith, J.B. 1995. Murine lupus glomerulotropic monoclonal antibodies exhibit differing specificities but bind via a common mechanism. *J. Immunol.* **155**:2258–2268.
32. Waters, S.T., et al. 2004. Breaking tolerance to double stranded DNA, nucleosome, and other nuclear antigens is not required for the pathogenesis of lupus glomerulonephritis. *J. Exp. Med.* **199**:255–264.
33. Mannik, M., Merrill, C.E., Stamps, L.D., and Wener, M.H. 2003. Multiple autoantibodies form the glomerular immune deposits in patients with systemic lupus erythematosus. *J. Rheumatol.* **30**:1495–1504.
34. Ekins, R.P. 1987. Multianalyte immunoassay. *J. Pharm. Biomed. Anal.* **1**:55–68.
35. Ekins, R., Chu, F., and Micallef, J. 1989. High specific activity chemiluminescent and fluorescent markers: their potential application to high sensitivity and 'multianalyte' immunoassays. *J. Biolumin. Chemilumin.* **4**:59–78.
36. Ekins, R., and Chu, F. 1992. Multianalyte microspot immunoassay: the microanalytical "compact disk" of the future. *Ann. Biol. Clin. (Paris).* **50**:337–353.
37. Borrebaeck, C. 2000. Antibodies in diagnostics: from immunoassays to protein chips. *Immunol. Today.* **21**:379–382.
38. MacBeath, G., and Schreiber, S. 2000. Printing proteins as microarrays for high-throughput function determination. *Science.* **289**:1760–1763.
39. Haab, B.B., Dunham, M.J., and Brown, P.O. 2001. Protein microarrays for highly parallel detection and quantitation of specific proteins and antibodies in complex solutions. *Genome Biol.* **2**:1–13.
40. Robinson, W.H., Steinman, L., and Utz, P.J. 2002. Proteomics technology for the study of autoimmune disease. *Arthritis Rheum.* **46**:885–893.
41. Robinson, W.H., et al. 2002. Autoantigen microarrays for multiplex characterization of autoantibody responses. *Nat. Med.* **8**:295–301.
42. Robinson, W.H., Steinman, L., and Utz, P.J. 2003. Protein arrays for autoantibody profiling and fine-specificity mapping. *Proteomics.* **3**:2077–2084.
43. Fouser, L.S., and Michael, A.F. 1987. Antigens of the human glomerular basement membrane. *Springer Semin. Immunopathol.* **9**:317–339.
44. Houser, M.T., Scheinman, J.I., Basgen, J., Steffes, M.W., and Michael, A.F. 1982. Preservation of mesangium and immunohistochemically defined antigens in glomerular basement membrane isolated by detergent extraction. *J. Clin. Invest.* **69**:1169–1175.
45. Miner, J.H. 1998. Developmental biology of glomerular basement membrane components. *Curr. Opin. Nephrol. Hyperten.* **7**:13–19.
46. Xie, C., Zhou, J.X., and Mohan, C. 2003. Enhanced susceptibility to nephritis in the lupus facilitating NZW strain. *Arthritis Rheum.* **48**:1080–1092.
47. Ehrenstein, M.R., Cook, H.T., and Neuberger, M.S. 2000. Deficiency in serum immunoglobulin (Ig)M predisposes to development of IgG autoantibodies. *J. Exp. Med.* **191**:1253–1258.
48. Samuels, J., Ng, Y.S., Coupillaud, C., Paget, D., and Meffre, E. 2005. Impaired early B cell tolerance in patients with rheumatoid arthritis. *J. Exp. Med.* **201**:1659–1667.
49. Yurasov, S. et al. 2005. Defective B cell tolerance checkpoints in systemic lupus erythematosus. *J. Exp. Med.* **201**:703–711.
50. Xie, C., Sharma, R., Wang, H., Zhou, X.J., and Mohan, C. 2004. Strain distribution pattern of susceptibility to immune-mediated nephritis. *J. Immunol.* **172**:5047–5055.
51. Mohan, C., Adams, S., Stanik, V., and Datta, S.K. 1993. Nucleosomes: a major immunogen for pathogenic autoantibody-inducing T cells of lupus. *J. Exp. Med.* **177**:1367–1381.
52. Shi, X., Xie, C., Kreska, D., Richardson, J., and Mohan, C. 2002. Genetic dissection of SLE: *Sle1* and *Fas* impact distinct pathways leading to lymphoproliferative autoimmunity. *J. Exp. Med.* **196**:281–292.
53. Bombardier, C., et al. 1992. Derivation of the SLEDAI: a disease activity index for lupus patients. *Arthritis Rheum.* **35**:630–640.
54. Weening, J.J., et al. 2004. The classification of glomerulonephritis in systemic lupus erythematosus revisited. *J. Am. Soc. Nephrol.* **15**:241–250.
55. Buyon, J.P., et al. 2005. The effect of combined estrogen and progesterone hormone replacement therapy on disease activity in systemic lupus erythematosus: a randomized trial. *Ann. Intern. Med.* **142**:953–962.
56. Petri, M., Buyon, J., and Kim, M. 1999. Classification and definition of major flares in SLE clinical trials. *Lupus.* **8**:685–691.